MicroRNA-24/MODY Gene Regulatory Pathway Mediates Pancreatic β-Cell Dysfunction

Yunxia Zhu,[1] Weiyan You,[1] Hongdong Wang,[1] Yating Li,[1] Nan Qiao,[1] Yuguang Shi,[2] Chenyu Zhang,[3] David Bleich,[4] and Xiao Han[1]

Overnutrition and genetics both contribute separately to pancreatic β-cell dysfunction, but how these factors interact is unclear. This study was aimed at determining whether microRNAs (miRNAs) provide a link between these factors. In this study, *miRNA-24* (*miR-24*) was highly expressed in pancreatic β-cells and further upregulated in islets from genetic fatty (*db/db*) or mice fed a high-fat diet, and islets subject to oxidative stress. Overexpression of *miR-24* inhibited insulin secretion and β-cell proliferation, potentially involving 351 downregulated genes. By using bioinformatic analysis combined with luciferase-based promoter activity assays and quantitative real-time PCR assays, we identified two maturity-onset diabetes of the young (MODY) genes as direct targets of *miR-24*. Silencing either of these MODY genes (*Hnf1a* and *Neurod1*) mimicked the cellular phenotype caused by *miR-24* overexpression, whereas restoring their expression rescued β-cell function. Our findings functionally link the *miR-24*/MODY gene regulatory pathway to the onset of type 2 diabetes and create a novel network between nutrient overload and genetic diabetes via *miR-24*. ***Diabetes*** **62:3194–3206, 2013**

Type 2 diabetes is one of the most common metabolic diseases in the world, typically characterized by absolute or relative insulin deficiency. Insulin production from pancreatic β-cells plays a vital role in maintaining glucose homeostasis in adult mammals. Factors encompassing overnutrition (glucotoxicity and lipotoxicity) and genetics (1–3) are responsible for pancreatic β-cell dysfunction, either by interfering with insulin secretion (4) or by reducing β-cell number through breaking the balance between β-cell growth and cell death (5,6). Multiple regulatory pathways connected to β-cell impairment have been widely documented, illuminating critical intracellular elements that negatively modulate β-cell mass and glucose-stimulated insulin secretion (GSIS) (7–10). A concerted action of specialized transcription factors, such as *Hnf1α*, *Hnf1β*, *Pdx1*, and *Neurod1*, is required for β-cell development, growth, and insulin gene expression. Monogenic diabetes, or maturity-onset diabetes of the young (MODY), is caused by mutations of these genes (*Hnf1α-MODY*, *Hnf1β-MODY*, *Pdx1-MODY*, *Neurod1-MODY*) (11–16). Alternatively, functional abnormalities of MODY genes contribute to nutrient overload or proinflammatory cytokine-associated β-cell failure (17–20). For example, reduced abundance and nuclear distribution of MODY transcription factors compromise insulin gene promoter activity, eventually leading to β-cell impairment (14,21–23). However, MODY gene dysregulation might involve other less well-understood molecular mechanisms.

MicroRNAs (miRNAs) are endogenous small, noncoding regulatory RNAs (~22 nt) that target the 3′ untranslated region (3′UTR) of messenger RNAs by repression of protein translation or by cleavage of mRNAs, resulting in diminished target protein production (24,25). In both plants and animals (26), miRNAs are estimated to influence ~30% of protein-coding genes (27–29). Accordingly, miRNAs have been implicated in many biological processes, including cell differentiation, cell proliferation, apoptosis, metabolism, and immune responses (30–32). However, specific functions have been identified only for a few miRNAs, and few reports have addressed these functions in β-cells (33,34).

Previously, miR-375 was found to play a significant role in endocrine pancreatic growth, development, and insulin secretion, whereby miR-375 knockout mice developed hyperglycemia with reduced β-cell mass and excess glucagon production (35). Other pancreatic β-cell regulators include miR-7, which was highly expressed in the endocrine pancreas (36), and miR34a/miR-146, which were upregulated in β-cells subject to lipotoxic stress (37). In addition, conditional deletion of Dicer1, a gene that controls miRNA processing, led to rapid hyperglycemia through the coordinated decrease in miR-24 and increase in two insulin gene transcriptional repressors, Sox6 and Bhlhe22 (38).

In this study, we identified a series of altered miRNAs in islets isolated from diabetic *db/db* mice compared with those of nondiabetic littermates. Among these miRNAs, *miR-24* was the most enhanced. Recent publications indicated that *miR-24* is consistently enriched during terminal differentiation of hematopoietic cell lines into a variety of lineages, during thymic development of naïve $CD8^+$ T cells, and during development of muscle and neuronal cells (39–41). However, the specific role of *miR-24* in β-cells is unknown. Previous reports have shown that increased *miR-24* inhibits cell cycle progression by directly repressing E2F2, Myc, and other cell-cycle genes in HepG2 cells, while elevated *miR-24* levels induce cellular apoptosis by reducing the bcl-2 protein expression level (40,42). *miR-24* is also involved in the hepatocyte nuclear factor-α–miRNA inflammatory feedback circuit to regulate hepatocellular oncogenesis (43).

Using the mouse insulin-secreting cell line (MIN6 cell) and isolated primary islets, we demonstrated that palmitate,

From the [1]Key Laboratory of Human Functional Genomics of Jiangsu Province, Jiangsu Diabetes Center, Nanjing Medical University, Nanjing, Jiangsu, People's Republic of China; the [2]Department of Cellular and Molecular Physiology, Pennsylvania State University College of Medicine, Hershey, Pennsylvania; the [3]State Key Laboratory of Pharmaceutical Biotechnology, School of Life Sciences, Nanjing University, Nanjing, Jiangsu, People's Republic of China; and the [4]University of Medicine and Dentistry of New Jersey-New Jersey Medical School, Newark, New Jersey.

Corresponding author: Xiao Han, hanxiao@njmu.edu.cn.

Received 29 January 2013 and accepted 4 June 2013.

DOI: 10.2337/db13-0151

This article contains Supplementary Data online at http://diabetes.diabetesjournals.org/lookup/suppl/doi:10.2337/db13-0151/-/DC1.

a free fatty acid (FFA), enhances *miR-24* expression. Ectopic expression of *miR-24* resulted in failure of β-cell function. Further exploration revealed several MODY genes as direct targets of *miR-24*, mediating its deleterious effects. Our findings establish a new perspective on *miR-24*/*MODY* genes in regulating β-cell function, particularly as a potential mechanism for acquired obesity/fatty acid–induced toxicity in type 2 diabetes.

RESEARCH DESIGN AND METHODS

Cell culture and transient transfection. The mouse pancreatic β-cell line MIN6 was used between passages 16 and 32 and cultured to 70% confluence in Dulbecco's modified Eagle's medium (DMEM) (Invitrogen, Carlsbad, CA) with 25 mmol/L D-glucose supplemented with 15% FBS (Invitrogen), 100 units/mL penicillin, 100 μg/mL streptomycin, 10 mmol/L HEPES, and 50 μmol/L β-mercaptoethanol (Sigma-Aldrich, St. Louis, MO). Cells were maintained in a Thermo tissue-culture incubator at 37°C with a 95% O_2/5% CO_2 atmosphere. Lipofectamine 2000 reagent (Invitrogen) was used to transfect MIN6 cells and primary islets. miRNA precursors (Ambion, Applied Biosystems, Foster City, CA) were mixed with Lipofectamine 2000 at a ratio of 10 pmol:0.5 μL miRNAs and Lipofectamine 2000. The final concentration of each miRNA in the transfection sample was 50 nmol/L according to the manufacturer's instructions. Cotransfection experiments were performed with a ratio of 0.25 μg plasmid:10 pmol miRNAs in 48-well plates. Transfection efficiency was consistently >90% for both MIN6 cells and primary islets.

Isolation of pancreatic islets. The human pancreatic islets used in this study were from the First Affiliated Hospital of Nanjing Medical University, Nanjing, China. All animal studies were performed according to guidelines established by the Research Animal Care Committee of Nanjing Medical University. Eight- and 12-week-old C57BL/KsJ-lepr^{db}/lepr^{db} (*db/db*) mice, nondiabetic littermate controls, and male ICR mice (weight, 20–25 g) were purchased from the National Resource Center for Mutant Mice Model Animal Research Center of Nanjing University. Islet isolation and culturing methods have been described previously (44).

Islets isolated from *db/db* mice or littermate controls were collected, and an aliquot was used for mRNA extraction (400 islets/group) while the remainder was transferred to sterile 6-well plates and cultured in RPMI 1640 containing 11.1 mmol/L glucose supplemented with 10% FBS, 100 units/mL penicillin and 100 μg/mL streptomycin. After equilibrating for 3 h, islets were replated into 48-well plates (8 islets/well), cultured for an additional 24 h, and then used for GSIS assays. Islets isolated from ICR mice were transferred to 6-well plates and cultured overnight at 37°C. The following morning, islets were transfected with 50 nmol/L of the prenegative control miRNA (pre-Neg) or pre–miR-24 for 48 h, and then replated into 48-well plates (8 islets/well) for GSIS assays. The remaining islets (~100) were used for RNA extraction.

RNAi, plasmid construction, and luciferase reporter assay. Silencing of Hnf1a and Neurod1 expression was performed using small interfering RNA (siRNA) duplexes purchased from Ribobio (Guangzhou, China) with the following sequences: Hnf1a sense, CGAAGAUGGUCAAGUCGUAdTdT; Hnf1a antisense, UACGACUUGACCAUCUUCGdTdT; Neurod1 sense, CGAAU UUCGUGUAGCUGUAdTdT; Neurod1 antisense, UACAGCUACACGAAAUU CGdTdT. The pGL3-basic vector (Promega, Madison, WI) was used to generate a luciferase reporter construct driven by the insulin promoter, as previously reported (40). To generate the wide-type (wt) 3′UTR-luciferase constructs of Neurod1, Kcnj8, and Kcnj11, the whole 3′UTRs (1.2, 0.6, and 1.4 kb) of the mouse Neurod1 (NM_010894.2), Kcnj8 (NM_008428.4) and Kcnj11 gene (NM_001204411.1) were amplified by PCR from genomic DNA and inserted into the pMIR-REPORT Luciferase vector (Ambion) between the *Sac*I and MluI, *Spe*I and *Hin*dIII, and *Spe*I and *Sac*I sites, respectively. Mutant (mt) construct of Neurod1 3′UTR in the miR-24 binding site was generated using QuikChange Site-Directed Mutagenesis kit (Stratagene). All of the sequences of miR-24 MREs were from the public source (miRanda, TargetScanmouse 4.2). Wt or mt sequences were obtained, synthesized, annealed, and subcloned into the *Spe*I and HindIII sites of the pMIR-REPORT vector. Luciferase activities were measured with a dual-luciferase reporter assay system (Promega). The *Firefly* luciferase activity was normalized with the *Renilla* activity of the PRL-SV40 plasmid (Promega). The mouse Neurod1 and Hnf1a expression plasmids were constructed by inserting the full-length coding region sequences into pCMV5-myc vector or pAdTrack-CMV vector. The mouse Ccnd3 and Cdk4 expression plasmids were constructed by inserting the full-length coding region sequences into pCMV5-myc vector as well. All constructions used here were sequenced and confirmed to be correct. Sequences of primers and oligonucleotides used for cloning are provided in Supplementary Table 1.

WST-1 assay. Cell viability was determined using WST-1 assays. Briefly, the cells were seeded in 48-well dishes (4×10^4 cells/well) in 200 μL culture medium and transfected with miRNAs mimics and inhibitors, as described above, for 48 h. Then, each well was supplemented with 20 μL WST-1 (Roche, Nonenwald, Germany) and incubated for 3 h in an incubator. The absorbance of the samples was measured with a spectrophotometer reader (wavelength 450 nm) against a background control (wavelength 630 nm) as blank. Data shown correspond to mean values from three independent experiments measured in $n = 6$ per experiment.

Flow cytometry analysis. MIN6 cells (1×10^6 cells/well) were cultured in 6-well plates and transfected with the indicated concentration of pre–miR-24 and pre-Neg for 48 h before cells were collected for flow cytometry analysis. The cells were harvested and fixed with 1 mL 75% ice-cold ethanol at −20°C overnight. After fixation, the cells were washed in PBS and stained with 500 μL propidium iodide solution (50 μg/mL) containing 25 μg/mL RNase. The cells were incubated at room temperature for 0.5 h in the dark and analyzed using a FACS Calibur flow cytometer and Cellquest Pro software (Becton Dickinson Immunocytometry Systems, San Jose, CA).

BrdU labeling assay. DNA synthesis was analyzed using the BrdU Labeling and Detection Kit I (Roche). Briefly, cells grown on coverslips in 24-well plates were transfected with miRNAs for 48 h. During the last 2 h, 10 μmol/L BrdU was added to each well. The cells were then processed according to the instructions provided with the labeling kit, except that in the final washing step, Hoechst 33342 (0.01 μg/mL, Sigma-Aldrich) was added to the wash reagent to stain all nuclei. Photographs of 10 random fields per coverslip were taken for the labeled cells using fluorescence microscopy. At least 800 cells were counted. The BrdU labeling index was defined as the ratio of the number of BrdU-positive nuclei to the total number of nuclei within the fields.

[^{3}H]thymidine incorporation assay. The incorporation of [^{3}H]thymidine into islet DNA was measured as described previously (39). Briefly, after isolation and overnight culture in 24-well plates as described above, the islets were transfected with 50 nmol/L pre-Neg or pre–miR-24 for 72 h. During the last 24 h, 37 kBq/mL of [methyl-^{3}H]thymidine (37 MBq/mL; Amersham Biosciences, Little Chalfont, U.K.) was added to each well. The islets were washed twice with PBS after the culture period and sonicated in 10 mmol/L Tris-HCl/5 mmol/L EDTA. DNA was precipitated by the addition of 10% ice-cold trichloroacetic acid and trapped by filtration on a GF/C glass-fiber disc (Whatman, Maidstone, U.K.). The discs were dried, and radioactivity was counted after the addition of scintillation fluid.

RNA extraction, microarray, and quantitative RT-PCR assays. MIN6 cells were cultured and treated as described above. Total RNA was extracted using Trizol reagent (Invitrogen). For mRNA microarray, total RNA samples were sent to Gene Tech (Shanghai, China) for analysis using Affymetrix GeneChip DNA microarrays. For miRNA quantification, stem-loop primers were designed with a short, single-stranded sequence complementary to the 3′-end of the miRNA, a double-stranded sequence (stem), and a loop containing the universal primer–binding sequence used for reverse primers. For mRNA determination, oligo-dT was used as reverse primers, and first-strand cDNA synthesis was performed using 1 μg total RNA (Promega). All RT-PCRs included no-template controls and RT minus controls. Quantitative (q)RT-PCR was performed using the SYBR Green PCR Master Mix and LighteCycler480 II Sequence Detection System (Roche, Basel, Switzerland). miRNAs were normalized with *U6*, and mRNA was normalized with *β-actin*. Sequences of the primers used are available in Supplementary Table 2. For *miR-24*, *miR-34a*, and *U6*, TaqMan probes purchased from Applied Biosystems (Carlsbad, CA) were used to confirm our results. Sequences of the primers used are available in Supplementary Table 2.

GSIS assay. MIN6 cells (2×10^6 cells/well) or isolated mouse islets (8 islets/well) were seeded in 48-well plates and transfected with miRNAs as above for 48 h for GSIS and potassium-stimulated insulin secretion (KSIS) assays. MIN6 cells or the islets were preincubated for 1 h in HEPES-balanced Krebs-Ringer bicarbonate buffer (KRBH) containing 2 mmol/L glucose and 1 g/L BSA. The islets or MIN6 cells were incubated for 1 h in KRBH containing basal glucose (2 mmol/L), stimulatory glucose (20 mmol/L), or KCl (50 mmol/L). After the static incubation period, supernatants were collected and frozen at −70°C for subsequent determination of insulin concentration. The insulin levels were measured using a radioimmunoassay as described previously (44).

Western immunoblotting. MIN6 cells were cultured and treated as described above and lysed with ice-cold lysis buffer containing 50 mmol/L Tris-HCl (pH 7.4), 1% NP-40, 150 mmol/L NaCl, 1 mmol/L EDTA, 1 mmol/L phenylmethylsulfonyl fluoride, and Complete protease inhibitor (1 tablet/10 mL; Roche). After protein content determination, Western blotting was performed as described previously (44). Individual immunoblots were probed with a mouse anti-Cdk4 monoclonal antibody (mAb), mouse anti-Cyclind3 mAb, rabbit anti-Cyclind1 polyclonal antibody (pAb), rabbit anti-p15 pAb, rabbit anti-Pten pAb, and rabbit anti-Parp1 pAb (Cell Signaling, Danvers, MA) diluted 1:1000; rabbit anti-Pdx1 pAb (Millipore, Billerica, MA) diluted 1:3000, rabbit anti-Hnf1a pAb

(Santa Cruz Biotechnology, Santa Cruz, CA) diluted 1:3000, rabbit antip27 pAb (Santa Cruz) diluted 1:1000, and goat anti-kir6.1 pAb (Santa Cruz) diluted 1:300 or goat anti-Neurod1 pAb (Santa Cruz) diluted 1:500. Target protein levels were quantified relative to levels of control protein, mouse anti–β-tubulin mAb, and mouse anti–β-actin mAb (Sigma-Aldrich) diluted 1:5000.

Statistical analysis. Comparisons were performed using the Student *t* test between pairs of groups or ANOVA for multiple group comparison. Results are presented as means ± SEM. A P value of < 0.05 was considered to be statistically significant.

RESULTS

Induction of *miR-24* by lipotoxicity in vivo and in vitro. To investigate the regulation of miRNA expression in the islets of diabetic mice, we used leptin receptor–deficient *db/db* mice as the animal model. The 8-week-old *db/db* mice exhibited high body weight, hyperglycemia, loss of GSIS, and reduced insulin synthesis compared with their littermate controls (Supplementary Fig. 1*A–E*). qRT-PCR was performed to quantify 13 highly expressed miRNAs in isolated islets from hyperglycemic *db/db* mice and euglycemic littermate controls (Fig. 1*A*). Consistent with previous reports, *miR-34a* and *miR-146a* were approximately twofold upregulated in *db/db* mice, whereas *miR-375* was downregulated by 70% compared with littermate controls. Among all these miRNAs, *miR-24* was highly upregulated from 2.0- to 3.5-fold in 8- and 12-week-old *db/db* mice (Fig. 1*B*). In vivo, primary islets isolated from

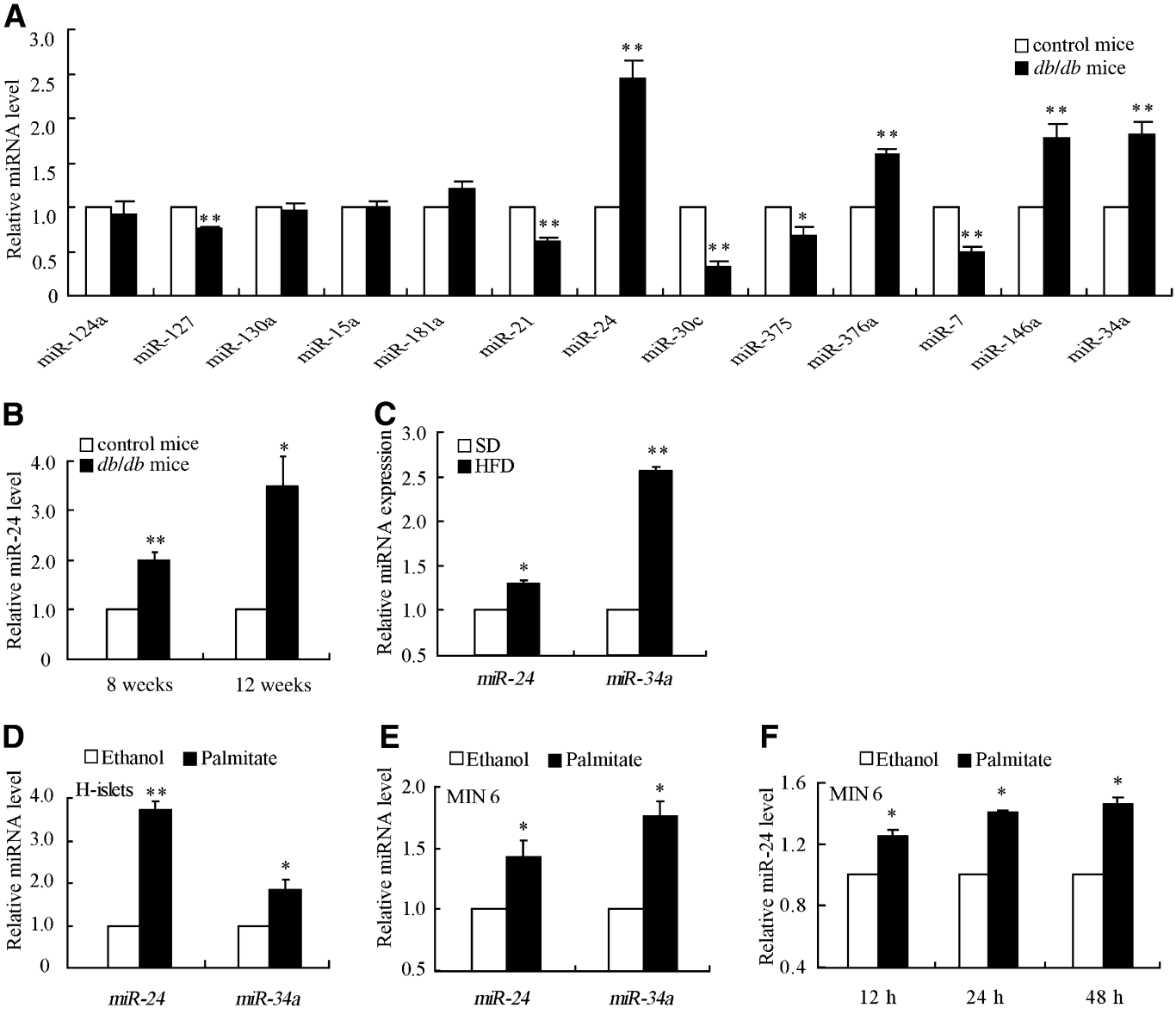

FIG. 1. Expression of *miRNA-24* is increased in pancreatic islet cells. *A*: Levels of 13 miRNAs in isolated islets from 8-week-old *db/db* mice (black) were analyzed relative to controls (white). Among them, *miR-127*, *miR-21*, *miR-30c*, *miR-375*, and *miR-7* were statistically significantly downregulated, whereas *miR-24*, *miR-376a*, *miR-146a*, and *miR-34a* were notably upregulated ($P < 0.05$). No changes were observed in *miR-124a*, *miR-130a*, *miR-15a*, and *miR-181a*. *U6* small nuclear RNA was used as an internal control to normalize miRNA expression (*$P < 0.05$ or **$P < 0.01$ vs. control mice). *B*: Islets from 8- and 12-week-old *db/db* mice and controls were isolated, and the expression of *miR-24* normalized to *U6* was measured using qRT-PCR (*$P < 0.05$ or **$P < 0.01$ vs. control mice). The expression of *miR-24* increased with age in the islets of *db/db* mice. Increasing expression levels of *miR-24* and *miR-34a* in islets from HFD-fed mice ($n = 5$) compared with controls fed the standard diet (SD) (*C*) (*$P < 0.05$ or **$P < 0.01$ vs. SD), palmitate-induced islets (*D*) (*$P < 0.05$ or **$P < 0.01$ vs. ethanol), and in palmitate-treated MIN6 cells (*E*) (*$P < 0.05$ vs. ethanol) were observed by TaqMan qRT-PCR relative to corresponding controls. *U6* detected by a TaqMan probe was used as an internal control. *F*: Levels of *miR-24* were upregulated in MIN6 cells challenged for various times (12, 24, and 48 h) with (black) or without (white) palmitate (*$P < 0.05$ vs. ethanol).

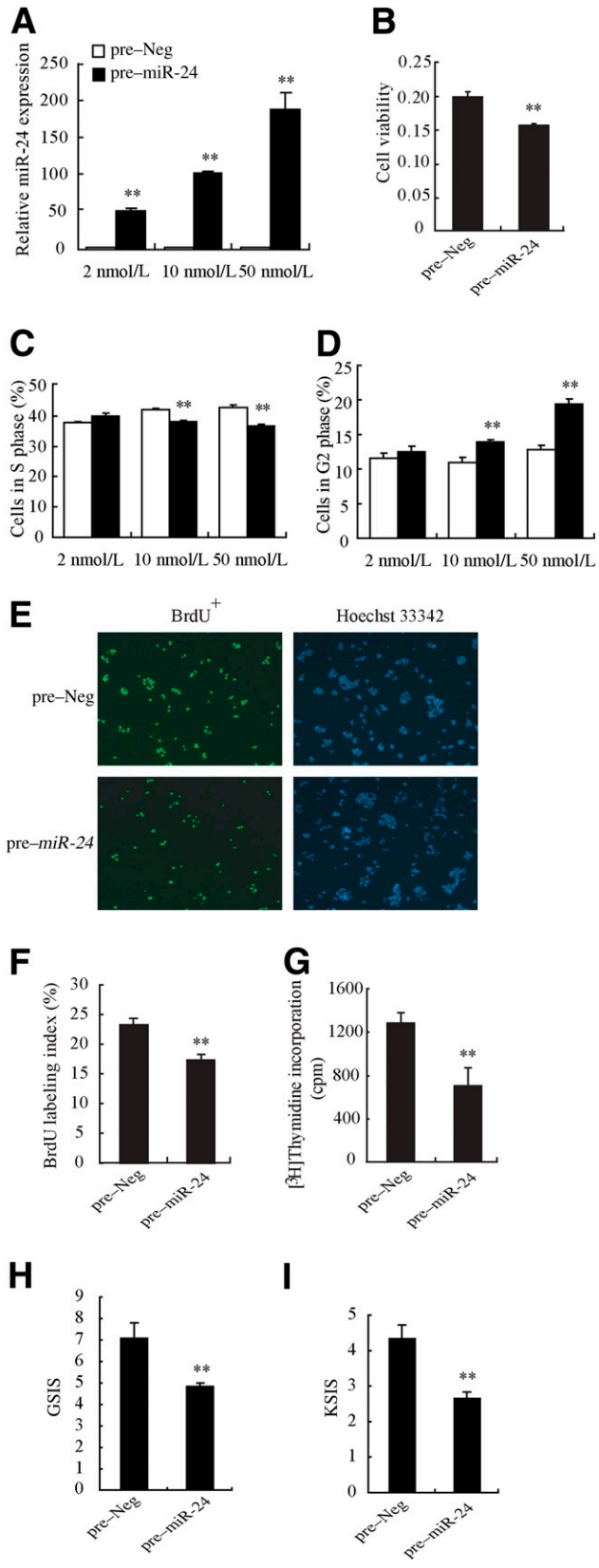

FIG. 2. Elevated *miR-24* reduces cell viability and impairs β-cell function. *A*: Pre–miR-24 mimetics or pre-Neg at different concentrations (2, 10, or 50 nmol/L) were transfected into MIN6 cells for 48 h, when TaqMan qRT-PCR was carried out. Transfection caused an effective increase in *miR-24* abundance in MIN6 cells. *B*: Overexpression of *miR-24* for 48 h caused a decrease of cell viability in MIN6 cells, measured by the WST-1 assay. Transfection of 10 nmol/L *miR-24* led to a decrease of cell number in the S phase (*C*) and to an increase in the G2 phase (*D*). The same results were detected with transfection of *miR-24* at 50 nmol/L but not at 2 nmol/L, which was insufficient to induce cell cycle arrest. *E* and *F*: BrdU labeling was used to confirm the reduced DNA synthesis accompanying the elevation of *miR-24*. *E*: Representative images show BrdU and Hoechst stained cells, and at least 800 cells were counted. *F*: The BrdU labeling index is defined as the ratio of the number of BrdU$^+$ nuclei to the total number of nuclei within the fields. *G*: Decreased cell proliferation was also detected in primary islets isolated from ICR mice. GSIS and KSIS assays were performed on MIN6 cells overexpressing *miR-24* for 48 h, and the GSIS index (*H*) and KSIS index (*I*) were calculated. The results were similar to those in palmitate-treated cells. **$P < 0.01$ vs. pre-Neg.

wild-type (WT) C57B6/J mice fed a high-fat diet (HFD) for 12 weeks became enriched with *miR-24* and *miR-34a* compared with cohorts fed the standard diet (Fig. 1*C*). Isolated human pancreatic islets and MIN6 cells were treated for 48 h with or without palmitate. In vitro incubation with palmitate led to significant increases of *miR-24* and *miR-34a* in human islets (Fig. 1*D*) and in MIN6 cells (Fig. 1*E*). Moreover, induction of *miR-24* in MIN6 cells initiated at 12 h with palmitate treatment continued to rise thereafter (Fig. 1*F*). The elevation of *miR-24* coincided with defective GSIS and KSIS (Supplementary Fig. 2*A*–*D*) and decreased cell viability (Supplementary Fig. 2*E*).

Enhancing *miR-24* expression mediates pancreatic β-cell impairment. To identify the effects of elevated *miR-24* expression, we transfected pre–miR-24 or pre-Neg miRNA precursors into MIN6 cells. The *miR-24* level was significantly increased by varying pre–miR-24 concentrations from 2 to 50 nmol/L in transfections (Fig. 2*A*) for 48 h. The viability of MIN6 cells was significantly decreased (~72%) with transfection of *miR-24* at 50 nmol/L (Fig. 2*B*). The cell cycle distribution analysis by flow cytometry revealed that cell proliferation was reduced starting from 10 nmol/L of transfected *miR-24*, mainly due to G2 phase arrest (Fig. 2*C* and *D* and Supplementary Fig. 3*A*). The results were confirmed by using the BrdU incorporation assay. Cells stained with BrdU and Hoechst 33342 are shown in Fig. 2*E*. The proportion of BrdU$^+$ cells was diminished significantly upon overexpression of *miR-24* (Fig. 2*F*). The ability of *miR-24* to inhibit proliferation was also observed in primary mouse islets by using the [^{3}H]thymidine incorporation assay (Fig. 2*G*). In all of the experiments undertaken, no changes in the level of apoptotic cells were detected (data not shown). Taken together, these observations suggest that upregulation of *miR-24* expression reduces pancreatic β-cell number by inhibiting replication.

Next, overexpression of *miR-24* in MIN6 cells inhibited insulin secretion induced by both glucose and potassium, whereas basal insulin secretion was not altered (Supplementary Fig. 3*B* and *C* and Fig. 2*H* and *I*). Increasing *miR-24* resulted in a slight decrease in insulin promoter activity and mRNA level (Supplementary Fig.3*D* and *E*). However, no significant change of insulin content was observed when normalized to total protein concentration (data not shown). These data demonstrated that *miR-24* overexpression repressed stimulus-induced insulin secretion.

Downregulation of target genes by *miR-24* overexpression. To understand the multiple effects caused by the elevation of *miR-24*, we sought to identify the regulated targets and cellular pathways by comparing mRNA microarrays transfected with pre–miR-24 or pre-Neg. In total, 351 genes were downregulated at least 1.5-fold by *miR-24* overexpression (Supplementary Table 3). qRT-PCR validated 33 genes with

a greater than 2-fold change and 4 genes with changes in the range of 1.5- to 2-fold. Except for *Mycbp* ($P = 0.05$), all of the other 36 genes were significantly downregulated, thereby validating the microarray results (Supplementary Table 4). Gene ontology analysis for the 351 downregulated genes by DAVID Bioinformatics Resources 6.7 demonstrated that upregulation of *miR-24* reduced cell viability and decreased insulin secretion in response to external stimuli (Supplementary Fig. 4*A*–*C*), which correlated well with the phenotype observed after *miR-24* overexpression as described above. By combining results obtained with target prediction software, luciferase activity assays, and qRT-PCR assays, only 12 genes were confirmed to be downregulated by overexpressed *miR-24* via directly binding to its miRNA recognition element (MRE) in the 3′UTR of those transcripts (Supplementary Fig. 5*A*–*E*).

Hence, the reason for the downregulation of the other identified genes lacking *miR-24* binding sites in their 3′UTR required further exploration. Bioinformatic analysis of their promoter sequences revealed that MODY genes, particularly *Hnf1a* and *Neurod1*, localized on promoter regions of these genes. Meanwhile, *miR-24* seeds were on site of 3′UTR sequences of *Hnf1α-MODY*, *Hnf1β-MODY*, *Neurod1-MODY*, and *Pdx1-MODY* (Fig. 3*A*). To find out whether these four MODY genes were regulated by *miR-24*, WT and mutant reporter constructs of their 3′UTR, including *miR-24* MREs, were cloned downstream of a luciferase reporter gene. Cotransfection with *miR-24* decreased luciferase activities of the WT constructs, but no alteration of luciferase activities was observed with the mutant constructs (Fig. 3*B*). Only the mRNA levels of *Neurod1* and *Pdx1* were slightly downregulated (Fig. 3*C*), suggesting that *miR-24* reduced their protein levels by repressing translation.

In addition to the four MODY genes, two other transcriptional factors, Cdx2 and Parp1, were also analyzed (Fig. 3*A*–*C*). To verify the luciferase reporter activity observed with the short MRE sequences, the reporter construct with the full-length 3′UTR of the *Neurod1* gene was generated. As shown in Fig. 3*D*, a high degree of conservation is present in the aligned 3′UTR sequence of *miR-24* between species (mouse and human). Overexpression of *miR-24* inhibited the luciferase activity of WT *Neurod1* by 33% compared with cells transfected with an empty construct, whereas no change with mutant *Neurod1* was observed (Fig. 3*E*). The full-length 3′UTR of *kcnj8* and *kcnj11*, each of which included a potential *miR-24* MRE, was also cloned, but no significant changes in activity were detected (data not shown). These results indicated that *miR-24* recognized the 3′UTR of *Neurod1* and specifically repressed its expression. In agreement with results of the luciferase activity assay, Western blot analysis confirmed a reduced expression of Neurod1 in cells transfected with *miR-24* for 48, 72, or 96 h (Fig. 3*F*). The inhibition of Neurod1 by transfected *miR-24* was observed beginning at the dose of 10 nmol/L for 48 h (Fig. 3*G*). Together, these results suggest that *miR-24* may have indirect and pleiotropic effects on many genes by modulation of MODY gene transcripts.

Analysis of functional genes in pancreatic β-cells. To further study the phenotype of MIN6 cells transfected with *miR-24*, protein expression levels of a series of functional genes were detected (Fig. 4*A*), and transcriptional factors Hnf1a, Neurod1, Pdx1, and Parp1 were significantly downregulated. Cell cycle–associated genes, such as *Cdk4*, *Cyclind3*, and *p27*, were repressed, whereas *p15* was strikingly increased; meanwhile, no changes of *Cyclind1* and *Pten* were observed. *Kir6.1*, which plays a key role in insulin secretion, was unchanged. In addition, *Cyclind3*, *Cdk4*, and *p15* were altered in a time- and dose-dependent manner. mRNA levels were also changed concurrently with their protein levels (Fig. 4*D*). Moreover, *Cyclind3* and *Cdk4* were confirmed to be downregulated in primary mouse islets (Fig. 4*E*).

Knockdown of *Hnf1a* and *Neurod1* mimics effects of *miR-24* elevation. To assess the contribution of *Hnf1a* and *Neurod1* to the *miR-24* effects, silencing efficiencies of these molecules were examined at mRNA and protein levels (Fig. 5*A* and *B*). Combined knockdown of *Hnf1a* and *Neurod1* contributed to the downregulation of 14 genes, including those with a 3′UTR lacking the *miR-24* seed sequence, whereas the other 7 genes were not modified (Supplementary Table 4). *Hnf1a* and *Neurod1* were both capable of decreasing BrdU incorporation. As shown by the GSIS assay, basal and stimulated levels of insulin, normalized to total protein content, were both repressed after silencing of *Hnf1a* and *Neurod1* (Fig. 5*D*).

Overexpression of *Hnf1a* or *Neurod1* rescues β-cells from effects of *miR-24* elevation. To further explore the involvement of mouse *Neurod1* and *Hnf1a* in *miR-24*–mediated damage, plasmids encoding these genes were cloned. Overexpression of Neurod1 in MIN6 cells was detected and found to rescue the expression of Cdk4 decreased by elevated *miR-24* (Fig. 6*A*). Meanwhile, GSIS, KSIS, and BrdU labeling assays were done. Surprisingly, all of the impairment caused by *miR-24* overexpression was rectified (Fig. 6*B*–*D*). Overexpression of *Hnf1a* showed the same effects as those of *Neurod1* (Fig. 6*E*–*H*), whereas overexpression of both Cyclind3 and Cdk4 rescued the cell replication decreased by elevated *miR-24* (Supplementary Fig. 6*A*–*C*).

Knockdown of miR-24 in islets obtained from HFD-fed mice restores normal GSIS. In vitro exposure of islets to palmitate upregulated miR-24 and impaired GSIS and KSIS. To determine whether knockdown of miR-24 could rescue islets from HFD-induced dysfunction, we isolated islets from mice fed the HFD for 10 weeks and then transfected them with an anti-miR negative control (Anti-Neg) or anti–miR-24 inhibitor (Anti–miR-24). As shown in Fig. 7*A*–*C*, HFD-fed mice gained excess weight and had elevated fasting glucose, and isolated islets demonstrated impaired GSIS compared with islets from control-fed mice. Islets obtained from HFD-fed mice were transfected with a Cy3-labeled Anti-Neg construct, and transfection efficiency was determined to be >90% when islets were counted under a fluorescent microscope (Fig. 7*D*). The elevated miR-24 in islets from HFD-fed mice was significantly downregulated by Anti–miR-24 transfection (Fig. 7*E*). Meanwhile, treatment of islets from HFD-fed mice with Anti–miR-24 restored robust GSIS compared with HFD islets treated with the Anti-Neg construct (Fig. 7*F*).

Oxidative stress increases miR-24 expression and inhibits miR-24 targets *Neurod1* and *Hnf1a*. Hyperglycemia and elevated FFAs both contribute to pancreatic β-cell dysfunction through mechanisms that increase oxidative stress. Pancreatic β-cells are exquisitely sensitive to reactive oxidation because they contain low levels of the free radical scavenging enzymes catalase, glutathione peroxidase, and superoxide dismutase. We subjected MIN6 cells to two forms of oxidative stress, hyperglycemia and hydrogen peroxide (H_2O_2), to demonstrate the effect on

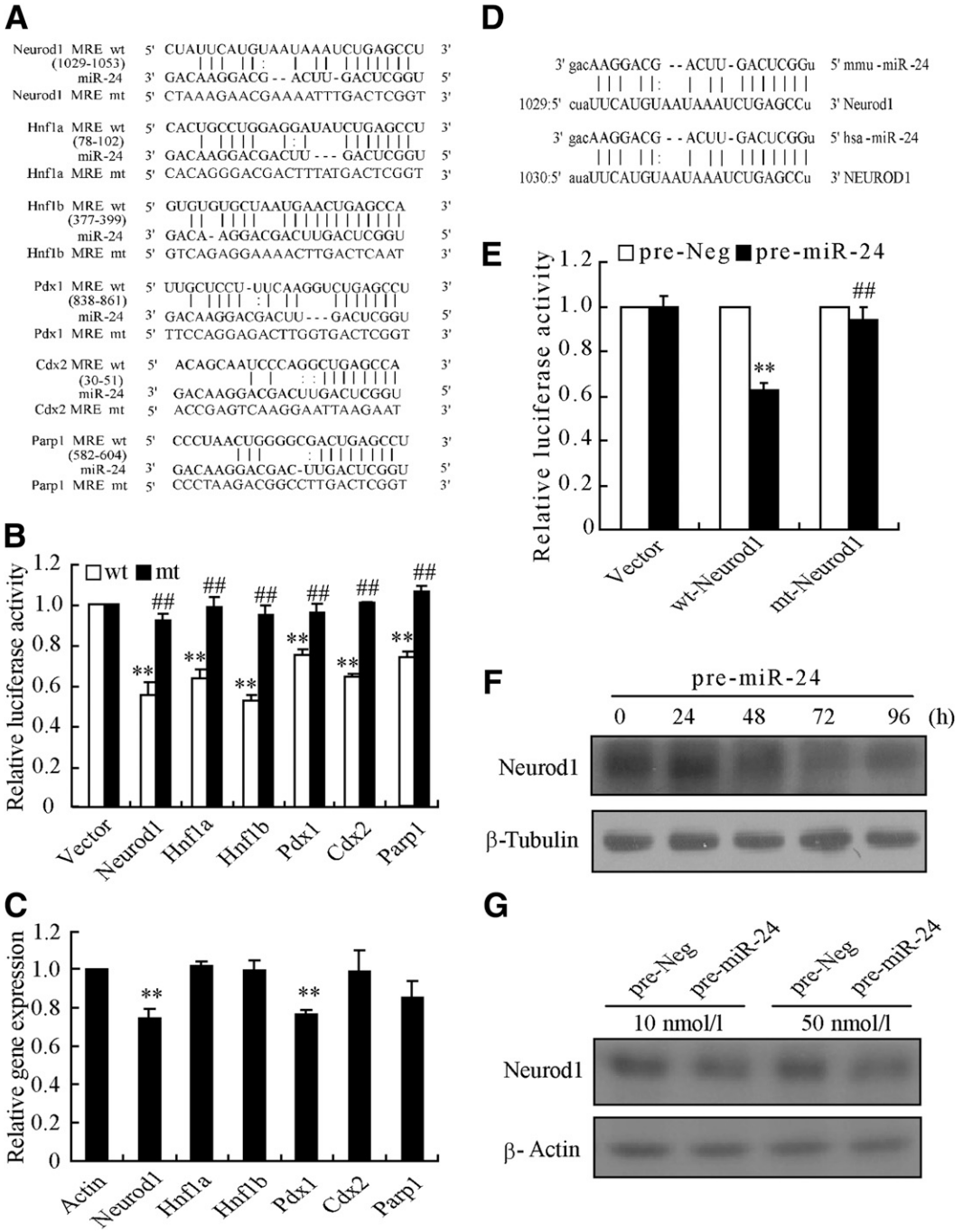

FIG. 3. *miR-24* directly downregulates six transcription factors. *A*: 3′UTR sequences of the six transcription factors predicted to include *miR-24* MREs were aligned with *miR-24*, and both WT and mutant sequences are listed. *B*: Luciferase reporter activities analyzed as above of WT gene promoters were significantly repressed by elevated *miR-24*, whereas those of the mutant gene promoters were reversed to the normal level ($P < 0.01$ vs. vector; ##$P < 0.01$ vs. wt). *C*: mRNAs analysis showed that only *Neurod1* and *Pdx1* were slightly downregulated, but others were not altered (**$P < 0.01$ vs. actin). *D*: Conserved *miR-24* binding sites in the 3′UTR of *Neurod1* from mouse and human. *E*: Full-length 3′UTR sequence of mouse *Neurod1* was inserted downstream of a reporter gene, and point mutation of the *miR-24* seed pairing sequence was generated using the QuikChange Site-Directed Mutagenesis kit. *miR-24* inhibited the luciferase activity of WT *Neurod1*, whereas those of the mutant construct and vector control were indistinguishable from each other (**$P < 0.01$ vs. vector+pre–miR-24; ##$P < 0.01$ vs. wt-Neurod1+pre–miR-24). *F*: *miR-24* (50 nmol/L) apparently decreased the Neurod1 protein level starting from 48 h. *G: miR-24* at both 10 and 50 nmol/L were sufficient to repress Neurod1 protein production.**

miR-24 and downstream targets *Hnf1a* and *Neurod1*. As shown in Fig. 8*A* and *B*, hyperglycemia and H_2O_2 both caused an increase in miR-24 expression by ~1.6- to 1.8-fold. In Fig. 8*C* and *D*, we quantified protein levels of MODY transcription factors *Hnf1a* and *Neurod1* using Western blot analysis. As shown, oxidative stress induced by H_2O_2 downregulated the Hnf1a protein level by twofold, while hyperglycemia downregulated both factors more than threefold.

DISCUSSION

Our findings, for the first time, demonstrate that *miR-24* mediates pancreatic β-cell dysfunction, linking lipotoxicity to type 2 diabetes. This pathway seems to be conserved from mouse to human islet cells and activated in islets from diet- and obesity-induced diabetic mice. The pathogenic effects of *miR-24* may occur when its level is sufficient to downregulate MODY genes, especially *Neurod1*

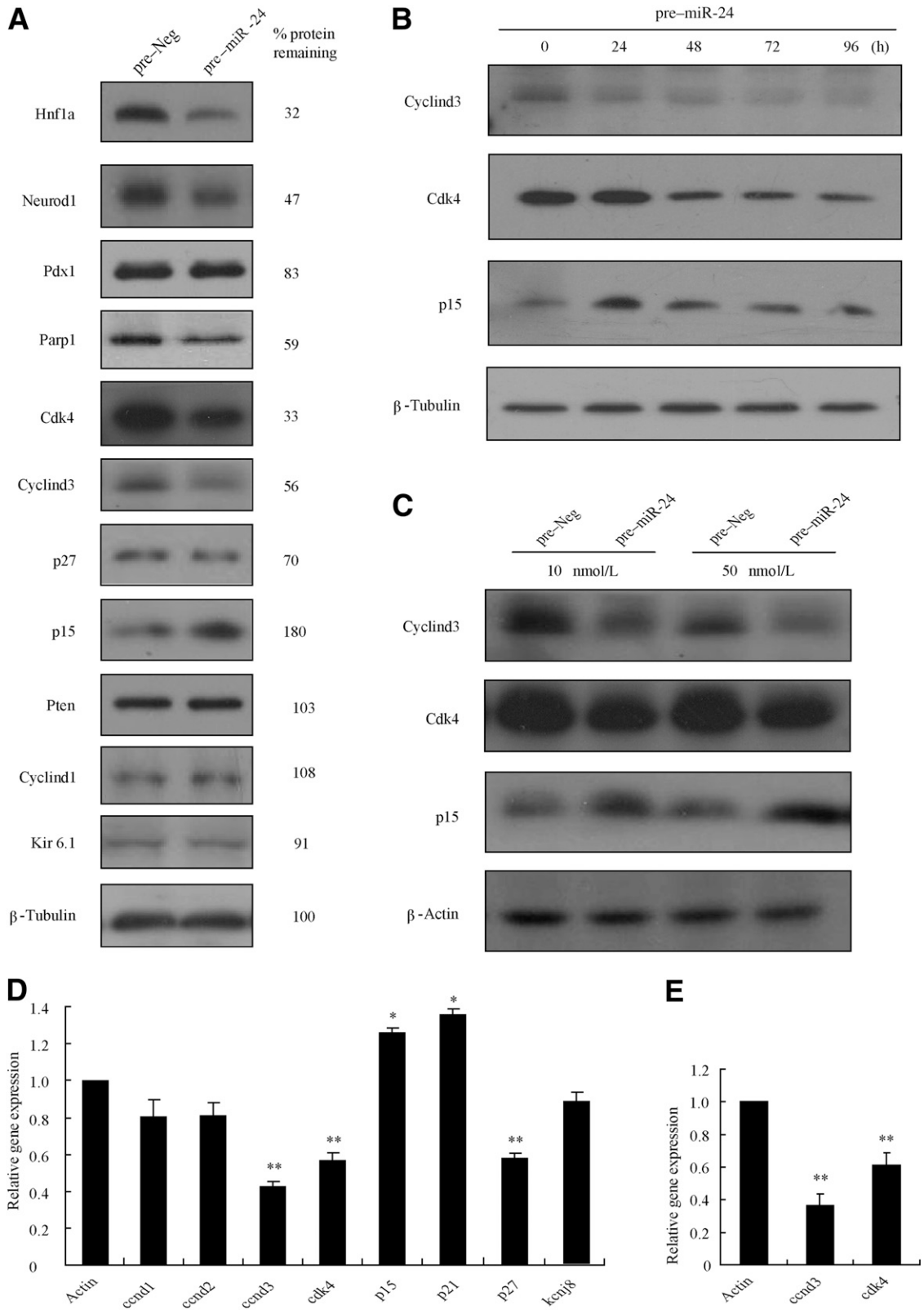

FIG. 4. Protein and mRNA level analysis of genes are functionally associated with *miR-24*. *A*: *miR-24* was transfected into MIN6 cells for 48 h, and then total protein was extracted for analysis of *Hnf1a*, *Neurod1*, *Pdx1*, *Parp1*, *Cdk4*, *Cyclind3*, *p27*, *p15*, *Pten*, *Cycind1*, *kir6.1*, and β-tubulin by Western blot. Protein levels remaining in cells relative to the negative control were quantitatively analyzed by Quantity One 4.2.1 (Bio-Rad). *B*: A decrease of *Cyclind3* was detected first at 24 h posttransfection of *miR-24* (50 nmol/L) and that for *Cdk4* was at 48 h. Meanwhile, the peak expression of p15 was at 24 h. *C*: Transfection with *miR-24* at 10 and 50 nmol/L downregulated *Cyclind3* and *Cdk4* protein levels and upregulated the *p15* level. *D*: Seven cell cycle–associated genes (*Ccnd1*, *Ccnd2*, *Ccnd3*, *Cdk4*, *p15*, *p21*, and *p27*) and genes of two components of ATP-sensitive potassium (K_{ATP}) channels (*Kcnj8* and *Kcnj11*) were determined by qRT-PCR. *Ccnd3*, *Cdk4*, and *p27* were decreased, whereas *p15* and *p21* were increased (P* < 0.05 or ***P* < 0.01 vs. actin). *E*: mRNA levels of *Ccnd3* and *Cdk4* were also downregulated in islets isolated from ICR mice (***P* < 0.01 vs. actin).**

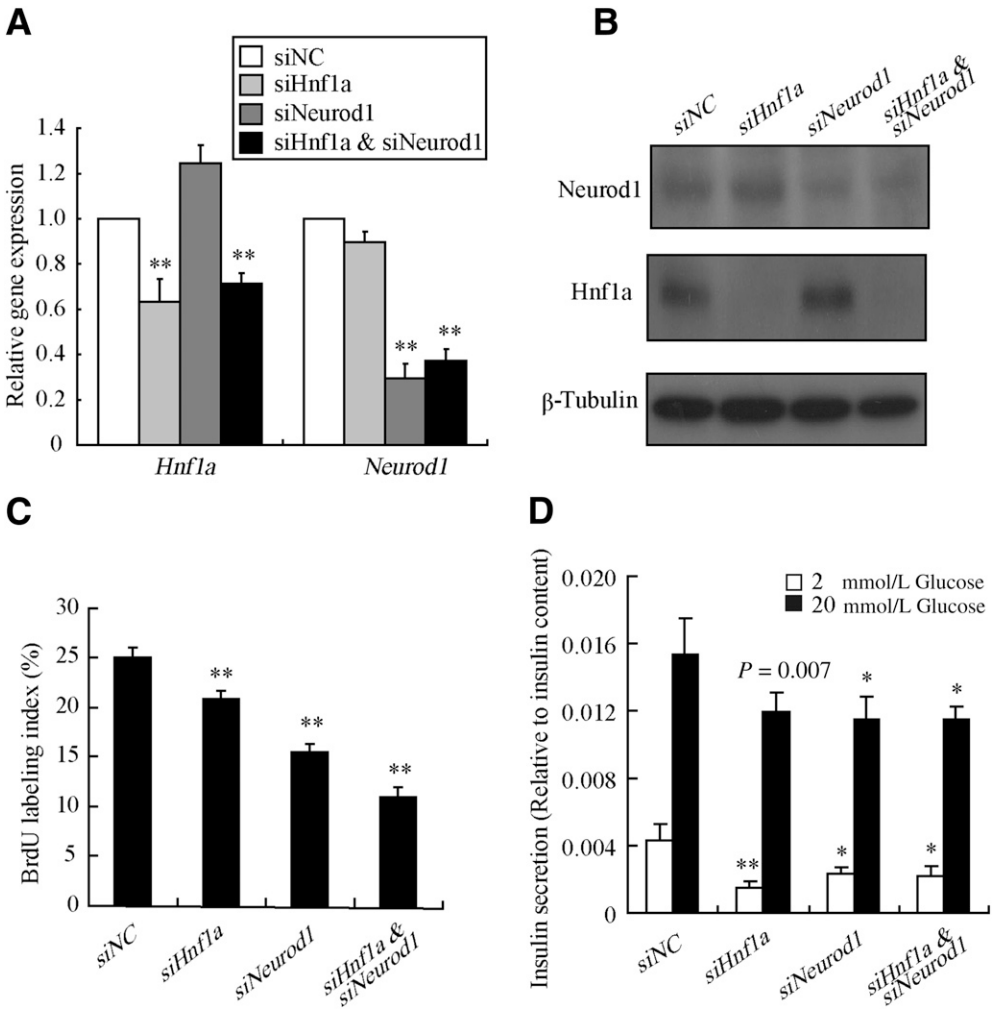

FIG. 5. Analysis of cellular phenotypes by silencing of *Hnf1a* and *Neurod1*. Silencing efficiencies of *Hnf1a* and *Neurod1* were measured at mRNA (*A*) and protein (*B*) levels using qRT-PCR and Western blotting, respectively (*P* < 0.01 vs. siNC). Results demonstrated that the siRNAs were effective. *C*: DNA synthesis was assessed by BrdU labeling. *Hnf1a* and *Neurod1* were both able to inhibit DNA synthesis, reflecting the capacity to reduce proliferation. This inhibition was enhanced by knocking down both proteins (***P* < 0.01 vs. siNC). *D*: GSIS assay was performed 48 h post-transfection of indicated siRNAs, and the released insulin was normalized to corresponding total insulin content. Basal and stimuli-induced insulin release were both repressed upon downregulation of *Hnf1a* or *Neurod1* (**P* < 0.05 or ***P* < 0.01 vs. siNC).**

and *Hnf1a*. Altering the protein level of *Neurod1* or *Hnf1a* blocks this pathogenic effect, indicating their leading roles in the effects of *miR-24*.

The epidemic of type 2 diabetes is mainly ascribed to nutrient overload and genetics. Human beings, as well as rodents, are predisposed to a combination of these factors (45) that culminate in pancreatic β-cell dysfunction. A number of studies have reported that inactivation of MODY genes, including *Hnf1a*, *Pdx1*, and *Neurod1*, induced by diet or FFA, individually or coordinately contributes to the onset of type 2 diabetes (15,16,21). However, the modulatory mechanism of defective MODY genes was unclear. Repressing translation and increasing mRNA degradation are two recognized ways to downregulate proteins at the post-transcriptional level (41,42). Because miRNAs effectively decrease protein synthesis in both of these ways, we sought to comprehensively investigate their functions in β-cells. In the current study, besides significantly increased *miR-146a* and *miR-34a* levels, consistent with previous reports, we identified another highly enhanced miRNA, *miR-24*. The abundance of mature *miR-24* was upregulated by palmitate in this study as well as by glucose previously (34), suggesting that *miR-24* is involved in the very early onset of type 2 diabetes. In contrast, conditional inactivation of the Dicer1 protein in pancreatic β-cells, a gene that controls miRNA processing, led to rapid hyperglycemia and impaired islet insulin content that was associated with decreased miR-24 (38). Here, decreased expression of miR-24 was shown to upregulate two insulin gene transcriptional repressors, Sox6 and Bhlhe22, thereby decreasing insulin gene transcription. These contradictory findings point at a highly complex set of regulatory networks that fine-tune β-cell insulin secretion and open up the possibility that a single miRNA might provide differential input as a member of one miRNA network compared with another network. Therefore, *miR-24* may play a critical role in both physiological and pathological conditions in β-cells through highly complex mechanisms that involve multiple levels of regulation.

In the current study, cDNA microarray analysis identified 351 genes downregulated by *miR-24*. Gene ontology enrichment analysis revealed that multiple biological processes, such as response to nutrients levels, vesicle-mediated

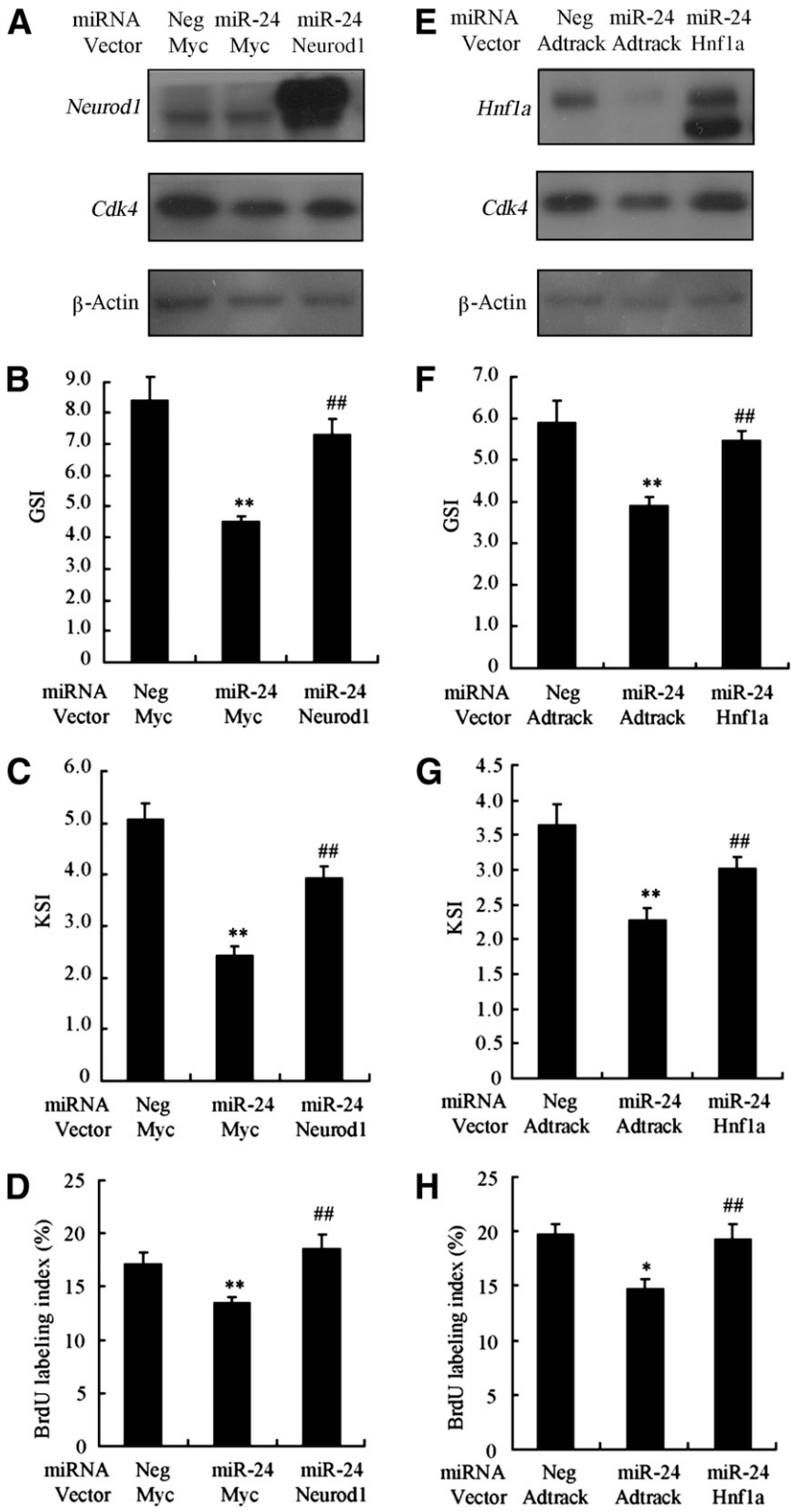

FIG. 6. Overexpression of *Neurod1* or *Hnf1a* blocked the cellular dysfunction induced by *miR-24*. Successful overexpression of *Neurod1* restored the *Cdk4* protein level (*A*), followed by the recovery of the GSIS index (*B*), KSIS index (*C*), and DNA synthesis (*D*) (*P* < 0.01 vs. Neg+myc; ##*P* < 0.01 vs. miR-24+myc). Overexpression of *Hnf1a* also helped to rescue *Cdk4* protein (*E*) as well as to restore the GSIS index (*F*), KSIS index (*G*), and DNA synthesis (*H*) (**P* < 0.05 or ***P* < 0.01 vs. Neg+Adtrack; ##*P* < 0.01 vs. miR-24+Adtrack).**

transport, and cell cycle control, were modulated, which agreed well with the *miR-24* overexpression phenotype. By combining computational and experimental analyses of 37 of these genes and by validating 13 direct targets of *miR-24*, we further found that MODY genes (*Hnf1a-MODY*, *Hnf1β-MODY*, *Neurod1-MODY*, and *Pdx1-MODY*) are directly modulated by *miR-24*, contributing to the decrease of the 14 *miR-24* seedless genes. Thus, we have

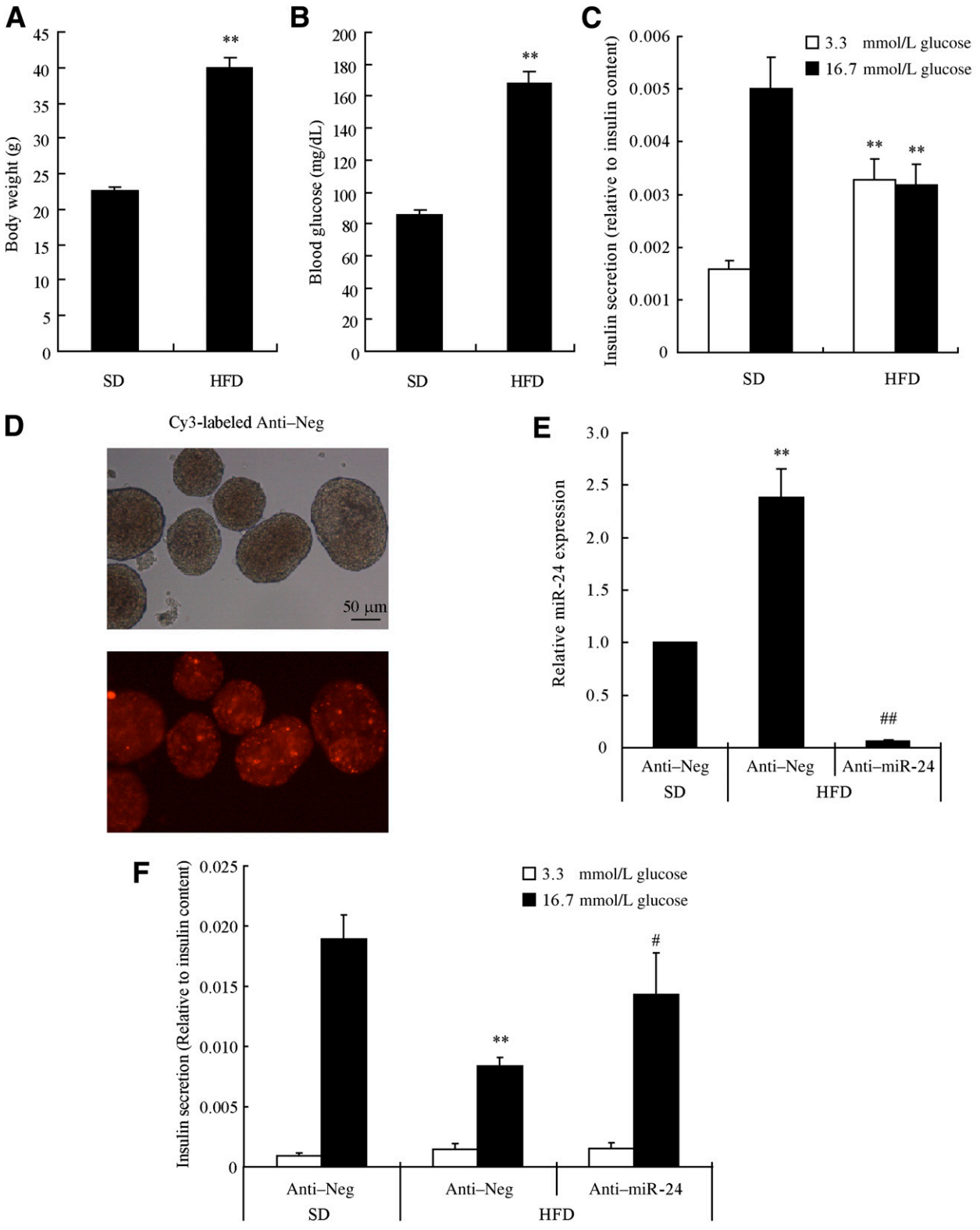

FIG. 7. Knockdown of miR-24 expression rescued the GSIS defect in islets from HFD-fed mice. C56BL/6 mice aged 8 weeks were fed an HFD or standard diet (SD) for 10 weeks. Mice were fasted for 8 h before measuring body weight (*A*) and blood glucose (*B*). Islets from HFD-fed mice (n = 9) and SD-fed mice (n = 16) were isolated and cultured for 3 h before GSIS (*C*) was performed. HFD mice exhibited high body weight, hyperglycemia, and defective GSIS compared with SD mice. Secreted insulin was normalized to relative insulin content (P < 0.01 vs. SD group). *D*: Islets from HFD mice were transfected with 100 nmol/L Cy3-labled Anti-Neg. After 48 h post-transfection, photographs of Cy3-labeled islets were acquired by fluorescent microscopy and used to quantify the transfection efficiency of miRNAs in primary isolated islets. After 3-h recovery in culturing medium, islets isolated from HFD mice were transfected with 100 nmol/L Anti-Neg or Anti-miR miRNA-24 inhibitor (Anti-miR-24) for 48 h, at which time qRT-PCR (*E*) and GSIS (*F*) were carried out. U6 was used as an internal control for miRNA analysis. Insulin secretion was normalized to relative insulin content (**P < 0.01 vs. Anti-Neg + SD; #P < 0.05 or ##P < 0.01 vs. Anti-Neg + HFD).**

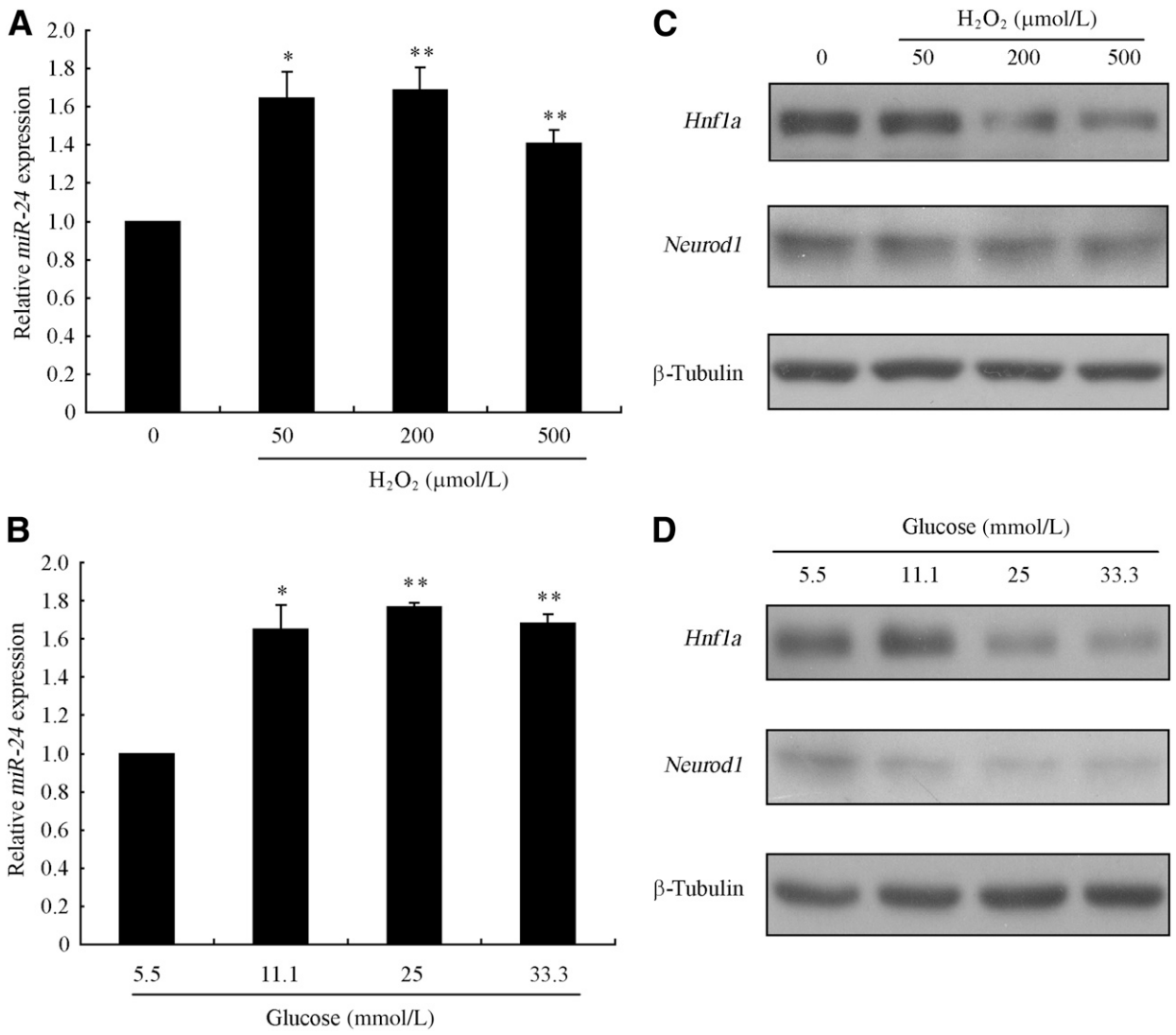

FIG. 8. Oxidative stress induced miR-24 expression. MIN6 cells were precultured in DMEM with 5.5 mmol/L glucose for 24 h, and then cells were incubated with the indicated concentration of H_2O_2 for an additional 24 h or with glucose for an additional 48 h. Relative expression of *miR-24* induced by H_2O_2 (*A*) or glucose (*B*) was analyzed by TaqMan qRT-PCR relative to corresponding controls. *U6* detected by a TaqMan probe was used as an internal control. Values are the mean ± SEM of three individual experiments (*$P < 0.05$; **$P < 0.01$). *C* and *D*: The protein levels of *Hnf1a* and *Neurod1* were observed by Western blotting. β-Tubulin was used as an internal control.

drawn a more comprehensive profile of *miR-24* downregulated genes. Existing publications generally have studied the relevance of one or two of those genes at most in the diabetic setting (14,16,21,23). Here, we demonstrated that *miR-24* coordinately targets four MODY genes, representing an efficient regulatory process.

Hnf1a and *Neurod1* previously were observed to be reduced in isolated primary islets under an HFD regimen (21). However, the potential mechanisms were unclear. Here, we established a connection between palmitate, *miR-24* elevation, and reduction of *Hnf1a* and *Neurod1* proteins. We described in detail the cause-and-effect relationship between the increased level of *miR-24* and decreased levels of *Hnf1a* and *Neurod1*. On the basis of the existing investigations, we speculated that *miR-24* was responsible for the reduction in *Hnf1a* and *Neurod1* proteins under the HFD condition. Although β-cell dysfunction caused by upregulation of *miR-24* was partially mimicked by silencing of *Hnf1a* and *Neurod1* and recovered by ectopic expression of *Neurod1* or *Hnf1a*, there were two phenotypic differences between these molecules. First, *miR-24* elevation only caused defective insulin secretion in response to stimulus, whereas silencing *Hnf1a* or *Neurod1* led to the deficiency in both basal and stimulated-insulin secretion. Second, although both factors decreased cell proliferation, they were associated with different cell cycle proteins; therefore, further study is needed to differentiate between the specific functions. Nevertheless, our results revealed that *miR-24* affects β-cell function mainly through modulation of *Hnf1a* and *Neurod1*. Although the use of MIN6 cells might invoke a note of caution in interpreting our results, we attempted to validate our targets in both mouse and human islets whenever possible.

Treatment with protein kinase C (PKC)/mitogen-activated protein kinase activators, a reactive oxygen species (ROS) generator, or transforming growth factor-β has been shown to increase *miR-24* expression (46,47). Nutrient overload and cytokines can induce ROS accumulation (20), and low levels of ROS are generated even in normal cells

(48). Therefore, the ROS/PKC pathway is likely to be activated in diabetic and possibly prediabetic patients, thus playing a potential role in β-cell dysfunction induced by an overload of nutrients such as palmitate (23,49,50). In our studies, oxidative stress led to upregulation of miR-24 and consequent inhibition of *Hnf1a* and *Neurod1*. Moreover, we showed that knockdown of miR-24 restored GSIS in islets obtained from HFD-fed mice, suggesting that miR-24 plays a central role in translating environmental oxidative stress from FFAs to genomic regulation of β-cell insulin production through modulation of MODY transcription factors. Hence, we propose that FFA induces *miR-24* expression through the ROS/PKC signaling pathway, which may occur during the very early onset of diabetes. Although we did not investigate the influence of antioxidants on *miR-24* expression in this study, another report has revealed that the antioxidative drug *N*-acetylcysteine led to restoration of β-cell insulin production by upregulating *Hnf1a* protein levels (21).

In conclusion, our study reveals that *miR-24* is inducible by pathogenic factors of diabetes, thus leading to β-cell failure. Importantly, our results link overnutrition and reduction in MODY genes to the pathological effects in type 2 diabetes through elevation of *miR-24*. This study provides a more comprehensive view of miRNAs, broadens our understanding of the pathophysiological development of diabetes, and exemplifies a fine-tuned regulatory network of miRNAs in disease.

ACKNOWLEDGMENTS

This work was supported by grants from the National Basic Research Program of China (973 program, 2011CB504003) to X.H. and by the National Natural Science Foundation of China (81130013).

No potential conflicts of interest relevant to this article were reported.

Y.Z. researched data and participated in writing the manuscript. W.Y., H.W., Y.L., and N.Q. researched data. Y.S. and C.Z. contributed to discussion. D.B. participated in writing and editing the manuscript. X.H. provided oversight for project, participated in writing the manuscript, and edited the manuscript. X.H. is the guarantor of this work and, as such, had full access to all the data in the study and takes responsibility for the integrity of the data and the accuracy of the data analysis.

REFERENCES

1. Wajchenberg BL. beta-Cell failure in diabetes and preservation by clinical treatment. Endocr Rev 2007;28:187–218
2. Lindgren CM, McCarthy MI. Mechanisms of disease: genetic insights into the etiology of type 2 diabetes and obesity. Nat Clin Pract Endocrinol Metab 2008;4:156–163
3. Leroith D, Accili D. Mechanisms of disease: using genetically altered mice to study concepts of type 2 diabetes. Nat Clin Pract Endocrinol Metab 2008;4:164–172
4. Roccisana J, Reddy V, Vasavada RC, Gonzalez-Pertusa JA, Magnuson MA, Garcia-Ocaña A. Targeted inactivation of hepatocyte growth factor receptor c-met in beta-cells leads to defective insulin secretion and GLUT-2 downregulation without alteration of beta-cell mass. Diabetes 2005;54:2090–2102
5. Hao E, Tyrberg B, Itkin-Ansari P, et al. Beta-cell differentiation from nonendocrine epithelial cells of the adult human pancreas. Nat Med 2006;12:310–316
6. Rhodes CJ. Type 2 diabetes—a matter of beta-cell life and death? Science 2005;307:380–384
7. Cheung L, Zervou S, Mattsson G, et al. c-Myc directly induces both impaired insulin secretion and loss of β-cell mass, independently of hyperglycemia in vivo. Islets 2010;2:37–45
8. Kim HY, Kim K. Regulation of signaling molecules associated with insulin action, insulin secretion and pancreatic β-cell mass in the hypoglycemic effects of Korean red ginseng in Goto-Kakizaki rats. J Ethnopharmacol 2012;142:53–58
9. Yeom SY, Kim GH, Kim CH, et al. Regulation of insulin secretion and beta-cell mass by activating signal cointegrator 2. Mol Cell Biol 2006;26:4553–4563
10. Matsumura K, Chang BH, Fujimiya M, et al. Aquaporin 7 is a beta-cell protein and regulator of intraislet glycerol content and glycerol kinase activity, beta-cell mass, and insulin production and secretion. Mol Cell Biol 2007;27:6026–6037
11. Fajans SS, Bell GI, Polonsky KS. Molecular mechanisms and clinical pathophysiology of maturity-onset diabetes of the young. N Engl J Med 2001;345:971–980
12. Stride A, Hattersley AT. Different genes, different diabetes: lessons from maturity-onset diabetes of the young. Ann Med 2002;34:207–216
13. Hunter CS, Maestro MA, Raum JC, et al. Hnf1α (MODY3) regulates β-cell-enriched MafA transcription factor expression. Mol Endocrinol 2011;25:339–347
14. Wang L, Coffinier C, Thomas MK, et al. Selective deletion of the Hnf1beta (MODY5) gene in beta-cells leads to altered gene expression and defective insulin release. Endocrinology 2004;145:3941–3949
15. Kushner JA, Ye J, Schubert M, et al. Pdx1 restores beta cell function in Irs2 knockout mice. J Clin Invest 2002;109:1193–1201
16. Rubio-Cabezas O, Minton JA, Kantor I, Williams D, Ellard S, Hattersley AT. Homozygous mutations in NEUROD1 are responsible for a novel syndrome of permanent neonatal diabetes and neurological abnormalities. Diabetes 2010;59:2326–2331
17. Flatt PR, Green BD. Nutrient regulation of pancreatic beta-cell function in diabetes: problems and potential solutions. Biochem Soc Trans 2006;34:774–778
18. Newsholme P, Gaudel C, McClenaghan NH. Nutrient regulation of insulin secretion and beta-cell functional integrity. Adv Exp Med Biol 2010;654:91–114
19. Donath MY, Ehses JA, Maedler K, et al. Mechanisms of beta-cell death in type 2 diabetes. Diabetes 2005;54(Suppl. 2):S108–S113
20. Cnop M, Welsh N, Jonas JC, Jörns A, Lenzen S, Eizirik DL. Mechanisms of pancreatic beta-cell death in type 1 and type 2 diabetes: many differences, few similarities. Diabetes 2005;54(Suppl. 2):S97–S107
21. Ohtsubo K, Chen MZ, Olefsky JM, Marth JD. Pathway to diabetes through attenuation of pancreatic beta cell glycosylation and glucose transport. Nat Med 2011;17:1067–1075
22. Gu C, Stein GH, Pan N, et al. Pancreatic beta cells require NeuroD to achieve and maintain functional maturity. Cell Metab 2010;11:298–310
23. Hagman DK, Hays LB, Parazzoli SD, Poitout V. Palmitate inhibits insulin gene expression by altering PDX-1 nuclear localization and reducing MafA expression in isolated rat islets of Langerhans. J Biol Chem 2005;280:32413–32418
24. Falus A, Molnár V. Closer to the completed unity: messenger and microRNA profiling. An introduction. Semin Cancer Biol 2008;18:77–78
25. Wang M, Xie H, Mi S, Chen J. Recent patents on the identification and clinical application of microRNAs and target genes. Recent Pat DNA Gene Seq 2007;1:116–124
26. Zhang B, Wang Q, Pan X. MicroRNAs and their regulatory roles in animals and plants. J Cell Physiol 2007;210:279–289
27. Nilsen TW. Mechanisms of microRNA-mediated gene regulation in animal cells. Trends Genet 2007;23:243–249
28. Cuperus JT, Fahlgren N, Carrington JC. Evolution and functional diversification of MIRNA genes. Plant Cell 2011;23:431–442
29. Winter J, Jung S, Keller S, Gregory RI, Diederichs S. Many roads to maturity: microRNA biogenesis pathways and their regulation. Nat Cell Biol 2009;11:228–234
30. Alvarez-Garcia I, Miska EA. MicroRNA functions in animal development and human disease. Development 2005;132:4653–4662
31. Schickel R, Boyerinas B, Park SM, Peter ME. MicroRNAs: key players in the immune system, differentiation, tumorigenesis and cell death. Oncogene 2008;27:5959–5974
32. Zhao E, Keller MP, Rabaglia ME, et al. Obesity and genetics regulate microRNAs in islets, liver, and adipose of diabetic mice. Mamm Genome 2009;20:476–485
33. Pullen TJ, da Silva Xavier G, Kelsey G, Rutter GA. miR-29a and miR-29b contribute to pancreatic beta-cell-specific silencing of monocarboxylate transporter 1 (Mct1). Mol Cell Biol 2011;31:3182–3194
34. Tang X, Muniappan L, Tang G, Ozcan S. Identification of glucose-regulated miRNAs from pancreatic beta cells reveals a role for miR-30d in insulin transcription. RNA 2009;15:287–293
35. Poy MN, Hausser J, Trajkovski M, et al. miR-375 maintains normal pancreatic α- and β-cell mass. Proc Natl Acad Sci U S A 2009;106:5813–5818

36. Bravo-Egana V, Rosero S, Molano RD, et al. Quantitative differential expression analysis reveals miR-7 as major islet microRNA. Biochem Biophys Res Commun 2008;366:922–926
37. Lovis P, Roggli E, Laybutt DR, et al. Alterations in microRNA expression contribute to fatty acid-induced pancreatic β-cell dysfunction. Diabetes 2008;57:2728–2736
38. Melkman-Zehavi T, Oren R, Kredo-Russo S, et al. miRNAs control insulin content in pancreatic β-cells via downregulation of transcriptional repressors. EMBO J 2011;30:835–845
39. Zaidi SK, Dowdy CR, van Wijnen AJ, et al. Altered Runx1 subnuclear targeting enhances myeloid cell proliferation and blocks differentiation by activating a miR-24/MKP-7/MAPK network. Cancer Res 2009;69:8249–8255
40. Lal A, Pan Y, Navarro F, et al. miR-24-mediated downregulation of H2AX suppresses DNA repair in terminally differentiated blood cells. Nat Struct Mol Biol 2009;16:492–498
41. Neilson JR, Zheng GX, Burge CB, Sharp PA. Dynamic regulation of miRNA expression in ordered stages of cellular development. Genes Dev 2007;21:578–589
42. Lal A, Navarro F, Maher CA, et al. miR-24 Inhibits cell proliferation by targeting E2F2, MYC, and other cell-cycle genes via binding to "seedless" 3'UTR microRNA recognition elements. Mol Cell 2009;35:610–625
43. Hatziapostolou M, Polytarchou C, Aggelidou E, et al. An HNF4α-miRNA inflammatory feedback circuit regulates hepatocellular oncogenesis. Cell 2011;147:1233–1247
44. Zhu Y, Shu T, Lin Y, et al. Inhibition of the receptor for advanced glycation endproducts (RAGE) protects pancreatic β-cells. Biochem Biophys Res Commun 2011;404:159–165
45. Rossmeisl M, Rim JS, Koza RA, Kozak LP. Variation in type 2 diabetes—related traits in mouse strains susceptible to diet-induced obesity. Diabetes 2003;52:1958–1966
46. Takagi S, Nakajima M, Kida K, Yamaura Y, Fukami T, Yokoi T. MicroRNAs regulate human hepatocyte nuclear factor 4alpha, modulating the expression of metabolic enzymes and cell cycle. J Biol Chem 2010;285:4415–4422
47. Huang S, He X, Ding J, et al. Upregulation of miR-23a approximately 27a approximately 24 decreases transforming growth factor-beta-induced tumor-suppressive activities in human hepatocellular carcinoma cells. Int J Cancer 2008;123:972–978
48. Newsholme P, Rebelato E, Abdulkader F, Krause M, Carpinelli A, Curi R. Reactive oxygen and nitrogen species generation, antioxidant defenses, and β-cell function: a critical role for amino acids. J Endocrinol 2012;214:11–20
49. Eitel K, Staiger H, Rieger J, et al. Protein kinase C delta activation and translocation to the nucleus are required for fatty acid-induced apoptosis of insulin-secreting cells. Diabetes 2003;52:991–997
50. Tang C, Han P, Oprescu AI, et al. Evidence for a role of superoxide generation in glucose-induced beta-cell dysfunction in vivo. Diabetes 2007;56:2722–2731